

# Chain of Trust: Can Trusted Hardware Help Scaling Blockchains?

Hung Dang, Anh Dinh, Ee-Chien Chang, Beng Chin Ooi  
School of Computing  
National University of Singapore  
{hungdang, dinhhta, changec, ooibc}@comp.nus.edu.sg

## Abstract

As blockchain systems proliferate, there remains an unresolved scalability problem of their underlying distributed consensus protocols. Byzantine Fault Tolerance (BFT) consensus protocols offer high transaction throughput, but can only support small networks. Proof-of-Work (PoW) consensus protocol, on the other hand, can support thousands of nodes, but at the expense of poor transaction throughput. Two potential approaches to address these scalability barriers are by relaxing the threat model, or employing sharding technique to deal with large networks. Nonetheless, their effectiveness against data-intensive blockchain workloads remains to be seen.

In this work, we study the use and effectiveness of trusted hardware on scaling distributed consensus protocols, and by their extension, blockchain systems. We first analyze existing approaches that harness trusted hardware to enhance scalability, and identify their limitations. Drawing insights from these results, we propose two design principles, namely *scale up by scaling down* and *prioritize consensus messages*, that enable the consensus protocols to scale. We illustrate the two principles by presenting optimizations that improve upon state-of-the-art solutions, and demonstrate via our extensive evaluations that they indeed offer better scalability. In particular, integrating our optimizations into Hyperledger Fabric achieves up to  $7\times$  higher throughput, while enabling the system to remain operational as the network size increases. Another optimization that we introduce to Hyperledger Sawtooth allows the system to sustain high throughput as the network grows. Finally, our new design for sharding protocols reduces the cost of shard creation phase by upto  $35\times$ .

## 1. INTRODUCTION

Blockchain, the technology that underlies Bitcoin and several hundreds other crypto-currencies, is essentially a distributed, append-only ledger that stores ordered transactions. The ledger (or blockchain) consists of blocks forming a chain using cryptographic hash pointers, each block contains a sequence of transactions. The blockchain is maintained by a set of mutually distrusting nodes (often called replicas, or validators). These nodes run a distributed consensus protocol to guarantee the blockchain's consistency under arbitrary node failures.

Blockchain systems can be broadly classified as *permissioned* or *permissionless*. In the former, nodes are authenticated and they run Byzantine Fault Tolerance (BFT) protocols such as PBFT [16] to reach consensus. Permissioned

blockchains are being adopted by many industries for applications such as asset management [49], supply chain and settlement [6, 7]. However, BFT protocols are communication bound and have been shown not to scale beyond a dozen of nodes [22]. In a permissionless blockchain, any node can join the network, and the nodes run lottery-based (or Nakamoto) consensus protocols such as Proof of Work (PoW) or Proof of Stake (PoS) [50, 14]. The most well known application of permissionless blockchain is cryptocurrency, namely Bitcoin and Ethereum which run on PoW. These systems can support thousands of nodes, but at the expense of transaction throughput. For instance, Bitcoin can only process up to 7 transactions per second<sup>1</sup>.

One approach to overcome the scalability barrier of these consensus protocols is to use trusted hardware. Such hardware, for example Intel SGX [44], creates a secure (tamper proof and confidential) execution environment in which a trusted code base (or TCB) can run. The key idea behind this approach is to use the hardware to relax the Byzantine failure model, which can lead to better performance [40, 34]. Previous works [18, 39, 8, 61, 11] have shown that the hardware enables BFT protocols to tolerate  $f$  failures using only  $2f + 1$  replicas, as opposed to  $3f + 1$  without the hardware. Proof-of-Elapsed-Time (PoET) [5], recently introduced by Hyperledger Sawtooth, uses Intel SGX to completely replace Proof-of-Work (PoW). By avoiding the massive computation requirement in PoW, PoET expects to achieve high throughput.

Another approach is to use sharding, a common technique in distributed database systems that allows the system to scale by partitioning the network and the state. For instance, Elastico [41], OmniLedger [33] and Chainspace [9] divide the network into smaller committees (or shards) where each shard runs an independent BFT protocol. However, Elastico and OmniLedger require an expensive phase for forming the committees. Furthermore, all three solutions do not exploit trusted hardware, and they need hundreds of nodes per committee in order to ensure reasonable security.

In this paper, we address the problem of scaling blockchain systems with trusted hardware. Our focus is on scalability of BFT and PoW protocols which have been shown to be the performance bottleneck [22]. Instead of designing a new protocol from scratch, we take a principled approach that improves upon the state-of-the-art solutions. First, we conduct extensive experimental evaluations of consensus protocols that use trusted hardware. We quantify their performance against data-intensive blockchain workloads. For

<sup>1</sup><https://blockchain.info/stats>



Byzantine Fault Tolerance (PBFT) [16]. This protocol allows the nodes (or replicas) to agree on a sequence of requests to be executed. It consists of three phases: a *pre-prepare* phase in which the leader broadcasts a next request in a *pre-prepare* message, the *prepare* phase in which the replicas agree on the ordering of the request by sending out a *prepare* message, and the *commit phase* in which the replicas commit to the request and its order by sending out a *commit* message. Each node collects  $2f + 1$  *prepare* messages before moving to the commit phase, and executes the request only after it collects  $2f + 1$  *commit* messages. The leader is replaced by a *view change* protocol when replicas suspect leader failure. The protocol uses  $O(n^2)$  messages for  $n$  nodes, and it achieves both safety and liveness property. Other BFT protocols, for example [40, 34], extend PBFT to optimize for normal case (without view change) performance.

BFT protocols require  $n \geq 3f + 1$  nodes in order to tolerate  $f$  Byzantine failures. Their safety property is guaranteed under any network condition, i.e., fully asynchronous. On the other hand, liveness requires partially synchronous network, i.e., messages are delivered within an unknown yet finite bound. BFT’s safety implies consensus finality, meaning that once reached, consensus decision will not be changed.

### 2.1.2 Proof of Work protocol

PoW protocols assume a *permissionless* setting in which any node can join and leave the network at will [50, 56]. At a high level, the protocol randomly selects a leader who can propose the next block that the network will accept. This strategy of “one-say-all-adopt” requires a single round of multicast to reach agreement [50], alleviating the network communication bottleneck that PBFT and the likes observe, and allowing the network size to scale. Leader selection is a probabilistic process in which a node must show a proof in order to claim leadership. To ensure security, especially when an adversary can have multiple identities (e.g., sybil attacks [24]), the proof is a solution to a computational puzzle. The probability of solving the puzzle is proportional to the amount of computational power the node possesses over the total power of the network.

Being probabilistic, PoW cannot prevent multiple nodes from claiming leadership and proposing new blocks at the same time. It is possible to have two valid blocks extending from the same parent block, creating a fork in the blockchain. One common approach to resolve such a conflict is for the nodes to pick the longest branch of the fork, such that after some number of blocks, one branch will be adopted by the entire network with high probability.

PoW can scale to large number of nodes: 3000 and 4000 nodes for Bitcoin and Ethereum respectively [26]. However, its throughput is limited, e.g., 7 and 10 transactions per second in average<sup>3</sup>, due to the cost of PoW. The security model of PoW is different to that of BFT. In particular, it considers Byzantine tolerance in terms of threshold of the cumulative resource belonging to the Byzantine nodes, e.g., fraction of the total computational power, as opposed to the number of Byzantine nodes in BFT. Furthermore, safety property is dependent not only on Byzantine threshold, but also on network latency. More specifically, under a fully synchronous

<sup>3</sup><https://www.etherchain.org/>

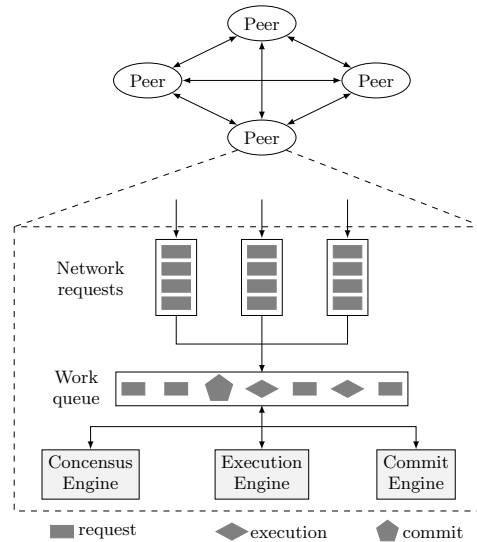


Figure 2: Hyperledger’s internal.

network (i.e., assuming zero network latency), safety is guaranteed against 50% Byzantine power [47]. However, this threshold drops quickly as network latency increases in a partially synchronous network, e.g., below 33% when the latency is equal to the block time [52]. Recent works consider the system of *rational* and Byzantine nodes as opposed to honest and Byzantine nodes in BFT. Under this model, PoW is more vulnerable to attacks such as selfish mining [25].

## 2.2 Intel Software Guard Extensions (SGX)

Intel SGX [44] is a recently introduced set of CPU extensions that provide hardware-protected trusted execution environment (or enclave). SGX allows a non-privilege process to create an enclave and run its code within. Both code execution and data inside the enclave cannot be seen or tampered with by the operating system, or any other untrustworthy processes. More specifically, an enclave is allocated a region of memory accessible by no other entities but the enclave owner. The code inside the enclave, however, can still make use of operating system services such as IO and memory management. Memory pages can be temporarily swapped out of the enclave memory, but they are encrypted before leaving the enclave.

SGX implements many cryptographic primitives in hardware, one of which is a random number generator called SGXRND. SGX provides an attestation service [10], allowing a remote user to verify that a specific enclave is running. This capability enables a remote enclave owner to establish a secure, authenticated channel with the enclave in order to transfer sensitive data.

## 2.3 Hyperledger Fabric

Hyperledger Fabric is a platform for permissioned blockchain applications. It contains an implementation of PBFT. It uses Docker to execute smart contracts, and a key-value store to persist the blockchain data. Its internal is depicted in Figure 2. Each node maintains fixed size queues to receive messages from other nodes. When a node receives a request from a client, it broadcasts to the rest of the network. Requests are forwarded to an internal work queue,

which are then picked up by the consensus engine. Once consensus is reached for a batch of requests (or a block), the batch is placed on the work queue to be executed by the execution engine. Results of the execution is placed to the work queue to be committed to the storage.

## 2.4 System and Threat Model

We assume a network of  $n$  nodes which are well connected. Unless otherwise stated, the network is partially synchronous in which messages sent repeatedly with finite time-out will eventually be received. Let  $f < n$  be the number of Byzantine nodes under the attacker’s control. We assume the remaining  $n - f$  nodes are honest. The attacker is computational bound, and it cannot break standard cryptographic assumptions. We assume the trusted hardware is secure against physical attacks that try to compromise its protection mechanisms. However, we do not consider side-channel attacks against the hardware.

## 2.5 Evaluation Setup

We used BLOCKBENCH [22] to generate blockchain workloads and drive the experiments. The workload contains read and write requests which are sent to a smart contract implementing a key-value store. We conducted the experiments using an in-house cluster of 48 servers, each equipped with E5-1650 3.5GHz CPU, 32GB RAM, 2TB hard drive, and running Ubuntu 14.04 Trusty. The servers are connected via a 1GB switch. We used Intel SGX SDK [2] to implement the trusted codebase. Since SGX is not available on the server hardware, we configured the SDK to run in simulation mode. We measured the latency of each SGX operation on Skylake 6970HQ 2.80 GHz CPU with SGX Enabled BIOS support, and injected it to the simulation. The results reported in the following sections are averaged over 5 independent runs.

## 3. SCALABLE DISTRIBUTED CONSENSUS PROTOCOLS REVISITED

This section presents an in-depth analysis of existing works on scaling distributed consensus protocols. Both BFT and PoW protocols are limited in their scalability, either in terms of the network size (i.e., number of nodes) or the overall throughput. The design space for improving them is vast. In this paper we focus on two design approaches, namely using trusted hardware and sharding. We discuss other related approaches in Section 6.

Table 1 summarizes the scaling proposals for consensus protocols that we examined in this paper. For each protocol, we first describe its design before presenting its performance evaluation. Then, we discuss the design choices that lead to limitations in the protocol’s scalability.

### 3.1 Scaling BFT

The most prominent BFT consensus protocol is the Practical Byzantine Fault Tolerance (PBFT) [16]. The original PBFT protocol requires  $n = 3f + 1$  nodes to tolerate upto  $f$  Byzantine failures, and incurs communication complexity of  $O(n^2)$ . This communication complexity hinders its scalability in term of network size. As a consequence, scaling proposals for PBFT focus either on reducing the number of nodes required to tolerate  $f$  Byzantine failures [18, 39, 11], or improving on the quadratic communication bound [32].

#### 3.1.1 AHL - Reducing the number of nodes

The complexity of PBFT, which is its need for three distinct phases, is necessary to ensure security when a Byzantine node can *equivocate*; i.e., issue conflicting statements to different nodes without being detected. To tolerate  $f$  Byzantine node that can equivocate in a quorum system like PBFT, quorums must be intersected by at least  $f + 1$  nodes [42]. As a consequence,  $n = 3f + 1$  nodes are needed to tolerate  $f$  failures.

Chun *et al.* [18] show that without equivocation, it is possible to tolerate  $f$  Byzantine failures with only  $n = 2f + 1$  nodes. As a result, the communication cost to tolerate the same number of failures becomes smaller than that of the original PBFT, due to smaller  $n$ . It also means that for the same number of nodes  $n$ , the network can tolerate more failures.

One way to eliminate equivocation is to run the entire consensus protocol inside a trusted enclave. This approach, adopted by Coco [8], effectively reduces the failure model from Byzantine to fail-crash. Thus, any non-Byzantine consensus protocols, such as Raft [51], can be used. However, this approach incurs a large trusted code base because of the complexity of the protocol. Chun *et al.* take another approach which only uses the trusted enclave to bind messages to sequence numbers that cannot be equivocated. Other works propose similarly simple trusted code bases [18, 39, 61, 11].

AHL is the implementation of PBFT-A2M [18] for Hyperledger. PBFT-A2M leverages the trusted log abstraction implemented in the hardware called attested append-only memory. The log can be appended, truncated and looked up. The operation and its results are cryptographically signed by the hardware, such that once a message is appended to a log it cannot be equivocated. AHL maintains different logs for different consensus message types, e.g., `prepare`, `commit`, `checkpoint` logs. Before sending out a new message, each node has to append its digest to the corresponding log. The proof of such append operation from the hardware is included in the message. The Byzantine node cannot forge the proof, hence it cannot equivocate about the log operation. In the normal case (without view change), each node collects and verifies  $f + 1$  `prepare` messages before moving to the commit phase, and  $f + 1$  `commit` messages before executing the request. However, the view change protocol in PBFT-A2M needs one extra round of communication, therefore it is more expensive than that in the original PBFT.

Other proposals, such as TrInc [39], MinBFT [61], CheapBFT [29] or Hybster [11], implement simpler abstraction of monotonic counters inside the hardware. They allow for binding a message with a certificate of trusted counter value. However, a faulty node can get two separate valid certificates for two conflicting messages. In this case, equivocation can only be detected when an honest node receives both certificates.

#### 3.1.2 AHLR - Reducing communication complexity

While reducing the network size needed for tolerating  $f$  failures, AHL has the same communication complexity of  $O(n^2)$ . This complexity is necessary because each node needs to collect authenticated messages from others in order to form quorums. Byzcoin [32] proposed an optimization wherein the leader uses a collective signing protocol

Table 1: Summary of existing scaling protocols evaluated in this paper.

	AHL [18]	AHLR [18, 32]	PoET [5]	Elsatico & Omniledger[41, 33]
Network	Permissioned	Permissioned	Permissionless	Permissionless
Trusted hardware	Yes	Yes	Yes	No
Design	Eliminate equivocation, requiring only $n = 2f + 1$ nodes to tolerate $f$ Byzantine failures [18]	Aggregate messages at the leader, reducing communication complexity to $O(n)$	Eliminate PoW by using SGX as trusted random source	Divide nodes into multiple shards, each shard runs PBFT

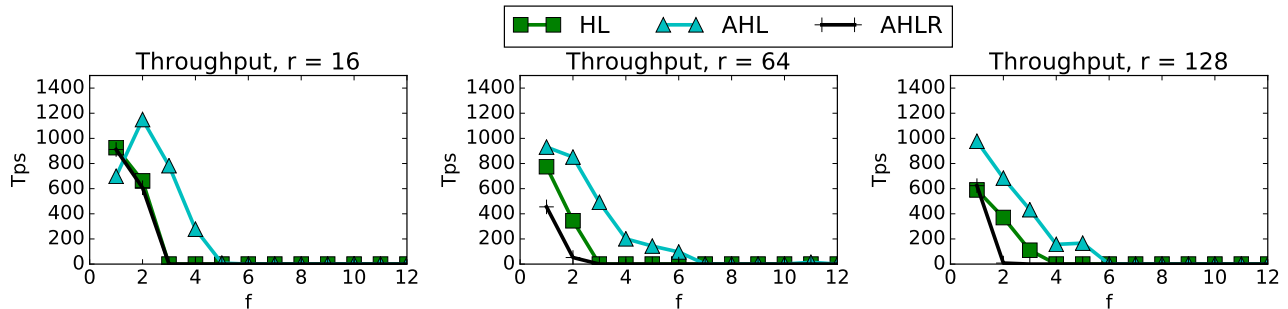


Figure 3: Throughput against increasing number of Byzantine failures.

(CoSi) [59] to aggregate other nodes’ messages into a single authenticated message. In this way, each node only needs to forward its messages to the leader, and verify the aggregate message from the latter. By avoiding broadcasting, the communication is reduced to  $O(n)$ .

AHLR adds collective signing to AHL. But instead of implementing the complex CoSi protocol, it relies on the trusted hardware to implement an enclave E-AGGRSIGN that performs message verification and aggregation (Algorithm 1). In particular, upon receiving  $f + 1$  signed messages for a request  $r$ , at a particular phase  $p$  of consensus round  $s$ , it issues an authenticated proof  $M$  indicating that there has been a quorum for  $\langle r, p, s \rangle$ , with which other nodes can proceed to the next phase. We note that AHLR can be realized without increasing the TCB, but with increased computation and communication cost due to the complexity of CoSi.

### 3.1.3 Performance evaluation

We measure the throughput of HL, AHL and AHLR against increasing number of Byzantine failures. We launch one client per node, each uses 16 threads, each thread sends  $r$  transactions per second (tps). Figure 3 shows the throughput with varying  $f$  and  $r$ .

We observe that AHL has higher throughput than HL for small value of  $f$ , with peak throughput of 1200 tps compared to 900 tps. However, both protocols crash at  $f = 7$ , and HL crashes earlier at  $f = 4$ . These can be explained by the difference in network sizes. For a given  $f$ , AHL requires smaller  $n$  than HL ( $3f + 1$  vs  $2f + 1$ ), hence it incurs less communication overhead. However, the overhead remains a quadratic function of  $n$ , thus AHL eventually crashes when  $f$  is large enough.

The performance of AHLR is interesting. Since AHLR reduces the communication cost to  $O(n)$ , it is expected to scale better than AHL. But the opposite is observed. In par-

---

#### Algorithm 1 Message Aggregation Enclave.

---

```

procedure E-AGGRSIGN( $\langle m_1, m_2, \dots, m_{f+1} \rangle$ )
   $\langle r, p, s \rangle \leftarrow \text{PARSE}(m_1)$ ;
  for each  $m_i$  do
    if  $\text{PARSE}(m_i) \neq \langle r, p, s \rangle \vee \neg \text{SIGVERIFY}(m_i)$  then
      return  $\perp$ 
    end if
  end for
   $M \leftarrow \text{SIGN}(\langle r, p, s \rangle)$ ;
  return  $M$ ;
end procedure

```

---

ticular, AHLR’s throughput is worse than those of HL and AHL, and the protocol crashes even earlier than HL. Careful examination reveals that the AHLR communication pattern makes the leader a single point of failure. The intuition is that without multicasting, a message drop at the leader is more consequential because the rest of the network depends on the leader to make progress. If the leader fails to collect and multicast the aggregate message before the time out, the system triggers the view-change protocol which is expensive. Figure 4 demonstrates the number of view change messages observed in different protocols, showing that AHLR suffers more view changes. We derive in Appendix A an analytical model for the probability of triggering view changes in AHL and AHLR. The model suggests that AHLR communication pattern is less robust to network congestion in comparison with AHL. This leads the system to triggers repeated view changes, which consequently incapacitates the system.

**Discussion.** The performance of AHLR suggests that there are other factors beside asymptotic complexity that effect scalability. Figure 4 shows that as  $f$  increases, there are more view changes during which nodes stop processing re-

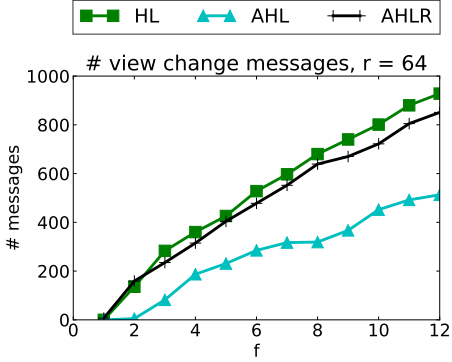


Figure 4: Number of view change messages.

quests. The large number of view changes demonstrates that the nodes get stuck in the view change phase. Indeed, view changes are triggered by two local timers: a request timer specifying an expected duration within which a request should be completed, and a view change timer indicating that of the view change phase.

We note that given a fixed network queue length (Figure 2), the probability of requests and consensus messages being dropped increases with  $f$ . A higher rate of message drop leads to more frequent triggering of view change. When it is high enough, the view change timer also fires repeatedly, i.e., the nodes are stuck in view change. One possible remedy is to lengthen the queue. However, no improvement is observed, because longer queues lead to longer processing time per request that exceeds the timer duration.

We examine the content of the network queue at each node, and observe that it has a disproportionate number of requests compared to consensus messages. We attempt to create a separate queue for consensus messages only, but the fact that the request queue keeps being filled did not lead to any performance improvement. We note that in PBFT’s formal specification [15], a non-leader node always broadcasts any request it receives. However, such broadcast is not necessary. That is, it only needs to forward the request to the current leader. The PBFT implementation in Hyperledger strictly follows the specification, thus it sends redundant multicast messages.

### 3.2 Proof-of-Elapsed-Time

PoW protocols are generally considered wasteful of resource. For example, Bitcoin network consumes up to 56TWh of electricity annually, which is more than most countries in Africa [1]. Hyperledger Sawtooth’s Proof of Elapsed Time (PoET) proposes a replacement to PoW that enforces a mandatory random wait time before a leader is elected.

PoET assumes that the nodes are equipped with Intel SGX CPU running a trusted enclave called E-PoET. At a high level, each node asks its E-PoET enclave for a *wait time*. Only after such wait time has passed does the enclave issue a *wait certificate* or create a new wait time. The node with the shortest wait time, i.e., the first to obtain a wait certificate, becomes the leader. The enclave generates the wait time as follows:

$$\text{waitTime} = \text{MinimumWait} - \text{localMean} \cdot \log(d) \quad (1)$$

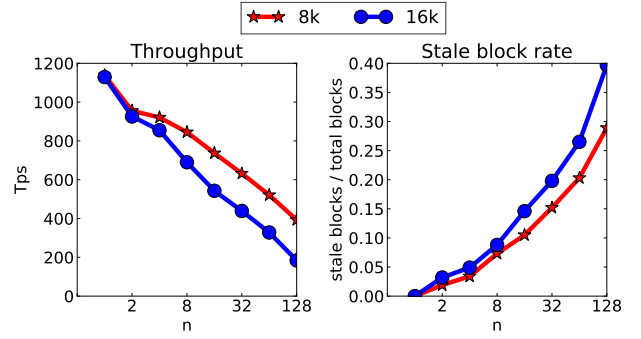


Figure 5: Throughput and stale block rate of PoET against exponentially increasing  $n$ .

wherein `MinimumWait` is a fixed system parameter, `localMean` is the product of expected block time and an estimated network size, and  $d \in (0; 1]$  is the hash value of the previous certificate [4]. Assuming that the hash function is a random oracle [30],  $d$  is a random seed. `localMean` is used to adapt `waitTime`’s deviation to the network size, i.e., larger network size leads to larger deviation and therefore lower probability of collision [17]. We note that both Bitcoin and Ethereum have similar self-adjusting mechanisms that adjust PoW difficulty to the network size.

The node attaches the wait certificate to the block it proposes, which will be adopted by the network if the certificate contains the shortest wait time. However, similar to PoW, PoET suffers from forks and stale blocks. Because of delays in blocks propagation, if multiple nodes get their certificates roughly at the same time, they will propose conflicting blocks, being unaware of the other. This conflict creates a fork in the blockchain, which is resolved as follows: the fork branch with highest *aggregate localMean* wins [3]. When the network size is fixed, PoET picks the longest branch. All other blocks not on the selected branch are discarded as stale blocks.

One effect of stale blocks is the overhead of verifying them, which can affect the overall throughput. A more important implication is security, i.e., the probability that a block is *unconfirmed* at a later time. PoET has similar security guarantee as other PoW protocols. In particular, with zero network latency, a transaction that has  $k$  block confirmations can only be unconfirmed with probability  $(\frac{r}{1-r})^k$  where  $r$  is the fraction of nodes that the attacker controls. As the network latency grows, the system tolerance reduces [53, 48]. In Bitcoin and Ethereum, the recommended value of  $k$  is 6 and 30 respectively. It remains unclear what the appropriate value for PoET is.

#### Performance evaluation

We evaluate performance of PoET based on Hyperledger Sawtooth v0.8 implementation by running up to 128 node instances on 32 physical servers<sup>4</sup>. Each node is connected to  $\sqrt{n}$  other nodes selected at random. We impose 50 Mbps limit to the bandwidth and 100ms latency on the network links. We observed through experimentation that a single node can validate upto 1150 tps, which serves as the upper bound of the system throughput. We vary the block size

<sup>4</sup>Each node instance runs on a separate CPU core.

from  $8k$  to  $16k$  transactions per block (i.e., 4MB to 8MB), and the corresponding block time from 8 to 16 seconds. Figure 5 shows the throughput and stale block rates against exponentially increasing  $n$ . We note that the throughput is not depicted against  $f$  as with PBFT. The reason is that PoET and other PoW protocols make assumption on network synchrony in order to achieve safety. Therefore in practice it is difficult to quantify their fault tolerance directly in terms of  $f$ . Although we did not compare PoET with Ethereum, due to their design differences, we note that PoET’s throughput is higher than Ethereum’s, which was reported in [22] to be around 100 tps for 32 nodes.

Recall that Eq 1 is expected to stabilize the throughput as network size increases. Instead, we observe a sharp drop of up to 82% (Figure 5[a]). This can be explained by the increased stale block rate (Figure 5[b]). More specifically, with more stale blocks, the node has to spend more time verifying them, thus ending up with less capacity for processing the valid blocks. We also observe that a larger block size leads to a higher stale block rate, and as a consequence, a lower throughput. This finding is in line with performance of Bitcoin network [20, 27], wherein larger block size means higher probability of forks and stale blocks.

**Discussion.** As stale block rate directly affects throughput, we consider its relationship with various system parameters: network size, block size and block time. We consider a simplified model in which message propagation delay has a lower bound  $\delta$ . Suppose  $n_1$  is the first to obtain the wait certificate, and it issues a block  $b_1$ . Suppose  $n_2$  obtains its wait certificate slightly after  $n_1$ , but before it receives  $b_1$ .  $n_2$  issues a block  $b_2$ , which will be conflicting with  $b_1$ . We note that conflicting blocks happen not only when the two nodes obtain the same wait time (which is rare), but also when their wait time difference is smaller than  $\delta$ . More specifically, let  $T$  be the average block time, then the probability of  $n_2$  proposing a conflicting block is  $\frac{\delta}{T}$ . In the network of  $n$  nodes, the expected number of conflicting blocks is  $C \approx \frac{n\delta}{T}$ .

Given the same block size and block time, i.e., fixing  $T$  and  $\delta$ , a larger network (i.e., larger  $n$ ) leads higher  $C$ . When block time increases linearly at the same rate as block size (in order to keep the expected throughput unchanged), we observed that  $\delta$  grows super linearly: 2.3s for 4MB blocks and 6.2s for 8MB blocks in a network of 128 nodes. This results in higher  $C$  when the block size increases.

### 3.3 Sharding Protocols

The distributed consensus protocols considered so far are leader based, which ultimately makes the leader’s processing capacity an upper limit of their overall throughput. To overcome this fundamental limitation, a common approach is to use sharding. A popular technique in database systems, sharding protocols partition the nodes (network partition) and the states (state partition) into smaller shards or committees. In the context of blockchain, sharding offers two benefits. First, each committee can be made reasonably small so that it is possible to run PBFT protocol among its nodes, which can achieve high throughput. Second, when there is light contention between transactions, the overall throughput can increase linearly with the number of committees. In other words, the throughput could scale linearly with the network size.

Three major sharding protocols for permissionless blockchains are Elastico [41], OmniLedger [33] and Chainspace [9]. Elastico uses network sharding, and assumes that there is no cross-shard transaction. Its sharding protocol splits the transactions per block to be processed in parallel by multiple committees. For each block, the miners perform PoW with low difficulty such that most miners can find a solution in reasonable time. The system specifies the number of committees as  $2^l$ , and two miners belong to the same committee if their PoW solutions share the last  $l$  bits. Transactions are forwarded to the corresponding committees based on their last  $l$  bits.

Unlike Elastico, OmniLedger splits the global states into multiple shards, thus a transaction may be cross-shard; i.e., it has to be processed by multiple committees. In OmniLedger, committees are fixed for a long period called epoch (e.g., a day). At each epoch, every nodes are known using a permissionless identity blockchain. At the beginning, one node is selected at random to serve as a *coordinator*, using a verifiable random function (VRF) [46]. Next, the coordinator drives the RandHound protocol [58] that collects inputs from the nodes and generates a fresh, non-bias random value. Figure 6 highlights key steps in RandHound. Using this random value, each node computes a random permutation  $\pi$  of  $[1..n]$ . To create  $k$  committees, the node divides  $\pi$  into  $m$  approximately equally-sized chunks, each chunk contains the IDs of the committee’s members. The global states are assigned to committees based on their last few bits. OmniLedger ensures consistency for cross-shard transactions by relying on a two-phase client-driven “lock/unlock” protocol.

Similar to OmniLedger, Chainspace partitions the global states into shards. However, it abstracts away the shard formation protocol and allows smart contracts to assign nodes to shards. Therefore, its security relies on such assignment to maintains 33% Byzantine threshold per shard. Chainspace uses a complex atomic commit protocol which incurs more cross-shard communication than OmniLedger. In this paper, we focus on Elastico and OmniLedger because of their secure shard formation protocols and simple cross-shard communication, and leave Chainspace to future work.

#### Performance Analysis

To ensure security of sharding, the nodes must be assigned to committees at random, otherwise the adversary could penetrate any committee in order to gain a majority. Both Elastico and OmniLedger assume synchronous communication during committee formation, wherein messages are delivered within a known bounded delay  $\Delta$ . They rely on unbiased randomness to form good committees. Elastico uses PoW as source of randomness, and therefore suffers from bias as miners can selectively discard PoW solutions to influence the result [13]. We examined the cost of RandHound for committee formation by running up to 512 node instances on 32 physical servers. Table 2 shows the latency with exponentially increasing  $n$  and  $c = 16$ . The cost of RandHound is significant, e.g., it takes nearly 3 minutes to generate a random value out of 512 nodes. We attribute this cost to the communication complexity of  $O(nc^2)$  [58].

Security of sharding protocols also depends on the committee sizes. In particular, the committee cannot be too small as the attacker can then become a majority and subvert the PBFT protocol. We define *committee failure* as the scenario in which a committee of size  $n'$  has more than

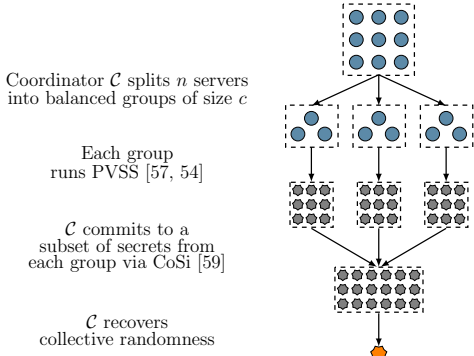


Figure 6: Illustration of RandHound protocol. The coordinator  $C$  generates fresh and bias-resistant randomness with inputs from multiple distrusting servers. The communication complexity is  $O(nc^2)$  where  $c$  is the size of groups generated in the first step.

Table 2: RandHound runtime with group size  $c = 16$ .

n	32	64	128	256	512
Time (s)	15.87	23.37	41.53	83.78	169.24

$\lfloor \frac{n'-1}{3} \rfloor$  Byzantine nodes. To tolerate attackers that control upto 25% nodes in the network (i.e., 25%-attackers), both Elastico and OmniLedger require more than 600 nodes per committee in order to keep committee failure probability below  $2^{-20}$ . Table 3 indicates that the required committee size grows almost exponentially if the network is to tolerate more failures. We remark that a 600-node network is too large for PBFT which is designed for much smaller networks (e.g., dozens of nodes).

Both the expensive committee formation phase, and the large committee sizes can be mitigated by trading off security. In particular, epochs can be made longer in order to reduce the frequency of forming new committees, amortizing the cost of committee formation. However, longer epochs make it easier for the attacker to adapt and compromise some committees. In addition, the Byzantine tolerance threshold can be lowered in order to use smaller committees. Our goal is to exploit trusted hardware to address the two limitations of sharding protocols without scarifying security guarantee.

## 4. DESIGN TO SCALE

In this section, we draw insights from the results presented in the previous section, and codify them into two design principles. Following these principles, we describe optimizations that improve AHL, AHLR and PoET. Finally, we present a new, efficient design for shard creation.

### 4.1 Design Principles

The performance analysis in the previous section gives us two insights. First, AHL, AHLR and PoET demonstrate a negative effect of network size on the overall throughput. These protocols essentially implement a replicated state machine (RSM) system which is driven by a leader. As such, the system performance is upper bounded by the leader's capacity, because the leader processes requests sequentially

Table 3: Required committee size against  $r\%$  attackers, to ensure failure probability below  $2^{-20}$ .

r	0	5	10	15	20	25	30
Committee size	1	28	55	106	227	648	4625

and the replicas merely follows. When the network size increases, message delay and message drop rate in AHL and AHLR grow larger, and the probability of nodes proposing conflicting blocks in PoET also become higher. In both cases, the overall throughput suffers.

The second insight is that frequent dropping of consensus messages in PBFT triggers repeated view change protocols and consequently paralyzes the system. Although it is expected that more messages are dropped as the number of nodes grows, we observed an unusually high drop rate in the Hyperledger Fabric implementation. The reason is that this implementation uses the same queue for both request and consensus messages. With more nodes, there are more requests filling up the network queue more quickly, causing consensus messages to be rejected. Worse still, every replica multicasts any request it receives to the rest of the network, further exacerbating the imbalance in the queue. This multicast is included in PBFT's formal specification as a means to ensure all the nodes receive the request [15]. However, this is unnecessary because the leader is already obliged to broadcast the request in the pre-prepare phase.

**Design Principle 1 - Scale up by scaling down.** This principle follows directly from the first insight. It recommends exploiting trusted hardware to reduce the number of nodes that take parts on the consensus, i.e., the *effective network size*. A smaller number of nodes means less communication overhead and lower rate of stable blocks, which translate to better throughput. The challenge is to maintain the same level of security as before scaling down. AHL and AHLR are examples of this principle, in which the effective network size is reduced from  $3f + 1$  to  $2f + 1$ .

**Design Principle 2 - Prioritize consensus messages.** Generalizing from the second insight, this principle recommends assigning importance scores to different types of messages, with consensus messages carrying the highest score. This could prevent consensus messages from being rejected from the queue or delayed after other message types.

### 4.2 AHL+: Prioritize Consensus Messages

Following the second principle, the drop rate of consensus messages should be minimized, which in the ideal case should be zero. To this end, we introduce the following optimizations to AHL. First, we divide the network queue into two parts: one for request, the other for consensus messages. By isolating the message types, consensus messages are never rejected. However, this alone did not deliver the improvement we expected, because the request queue is filled at a much higher rate than the consensus queue, causing long delay in processing the latter. In light of this, our second optimization removes request multicast at the replicas. In particular, upon receiving a request, the replica only forwards it to the leader, instead of broadcasting it to the network. Consequently, the request queue is filled at roughly the same rate as the consensus queue.



We note that the ideal optimization here is to maintain a priority queue out of consensus and request messages, and always giving higher priority to the former type. However, we opted not to introduce much change to the current Hyperledger code base, and implemented the more simple optimization above. As shown in the next section, even such simple optimization leads to significant improvement. Hence, we leave the priority queue implementation and evaluation to future work.

### 4.3 S-POET: Scaling Down the Effective Network

We apply the first principle to PoET in order to reduce the stale block rate, allowing the system to sustain a high throughput as the network size grows. More specifically, by having fewer nodes competing to propose the next block, i.e., smaller effective network, the expected number of conflicting block decreases<sup>5</sup>. To address the challenge of maintaining the security level, we exploit SGX to ensure that the effective network consists of nodes selected uniformly at random.

We introduce a small change to PoET trusted code base, and call the result S-POET. When invoked to generate a wait certificate, the enclave in S-POET also generates a random  $l$ -bit value  $q$  (using hardware-based random number generator SGXRNG). This value  $q$  is used to determine if the node belongs to the effective network. In particular, only wait certificates containing  $q = 0$  are considered valid. The node with a valid certificate and shortest wait time becomes the leader.

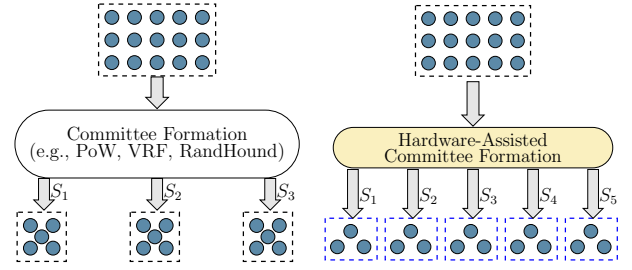
Without loss of generality, S-POET leader selection can be seen as a two-stage process. The first stage samples uniformly at random a subset of  $n' = n \cdot 2^{-l}$  nodes. The second stage selects uniformly at random a leader among these  $n'$  nodes. Following the model in Section 3.2, the expected number of stale blocks is  $C' \approx \frac{n'\delta}{T}$ , which is smaller than that of PoET. In addition, let  $r$  be the fraction of Byzantine nodes under the attacker’s control. In S-POET, the attacker gains no extra advantage, because its probability of becoming a leader is the same as in PoET, which is  $\frac{rn'}{n'} = r$ .

### 4.4 GRANBEA: Scaling-Out Sharding Protocols

Existing sharding protocols, namely Elastico and OmniLedger, follow our first design principle to some extent. They split the network into smaller committees and run an instance of PBFT within each committee. However, they use expensive protocols for committee formation, and the resulting are still too large for PBFT. We describe a new sharding protocol, called GRANBEA, that further follows the first design principle to address the above mentioned limitations without sacrificing security. A high level comparison of GRANBEA and the state-of-the-art is shown in Figure 7.

**Efficient committee formation.** Similar to OmniLedger, GRANBEA first collects a fresh, bias-resistant random value, and uses that random value to assign nodes into committees. GRANBEA avoids the overhead of RandHound protocol by replacing it with a trusted random beacon running inside a trusted enclave. For this phase, GRANBEA makes the same network assumption to that of OmniLedger and Elastico, i.e., the network is synchronous with the bounded delay  $\Delta$ .

<sup>5</sup>The effective network in PoET is the entire network of  $n$  nodes.



(a) Existing protocols with expensive committee formation and large committee size. (b) GRANBEA reduces committee formation cost and required committee size.

Figure 7: A high level comparison between state-of-the-art sharding protocols and GRANBEA. Nodes are split into shards. Each shard  $S_i$  runs an instance of BFT protocol to process its assigned transactions.

---

#### Algorithm 2 Hardware-Assisted Random Beacon.

---

```

procedure E-RANDGEN( $e$ )
  if LOAD( $e$ ) = false then
     $q \leftarrow$  SGXRNG();
     $\mathbf{rnd} \leftarrow$  SGXRNG();
    if  $q = 0$  then
       $c \leftarrow \langle e, \mathbf{rnd} \rangle$ ;
       $R \leftarrow$  SIGN( $c$ );
    else
       $R \leftarrow \perp$ 
    end if
    SAVE( $e, R$ );
    return  $R$ ;
  else
    return LOAD( $e$ )
  end if
end procedure

```

---

One naive solution to implement a trusted random beacon is to follow the design of PoET. More specifically, each node asks its enclave for a random value  $\mathbf{rnd}$ , and broadcasts it to the network. After  $\Delta$  has passed, all nodes lock in the *lowest*  $\mathbf{rnd}$  that they have seen. This solution incurs  $O(n^2)$  communication complexity.

Inspired by S-POET, our trusted random beacon, called E-RANDGEN and shown in Algorithm 2, samples uniformly at random a small number of nodes that could collect and broadcast  $\mathbf{rnd}$ . At the beginning of each epoch, each node invokes E-RANDGEN with an epoch number  $e$ . The enclave generates two random values  $q$  and  $\mathbf{rnd}$  using SGXRNG, and returns an authenticated certificate containing  $\langle e, \mathbf{rnd} \rangle$  only if  $q = 0$ . The enclave generates one certificate per epoch, preventing an attacker from selectively discarding the enclave’s output in order to influence final randomness. The certificate is broadcast to the network. After a time  $\Delta$ , every node locks in the *lowest*  $\mathbf{rnd}$  that it has seen for the epoch  $e$ , and uses it to compute the committee assignment. When failing to receive any message after  $\Delta$ , which happens when no node is able to collect a certificate from its enclave, the node increments  $v$  and repeats the process.

The bit length  $l$  of  $q$  defines the probability that the system fails to produce any random value (i.e., none of the nodes could collect  $\langle e, \mathbf{rnd} \rangle$ ) and hence has to repeat the process, which is  $P_{\text{repeat}} = (1 - 2^{-l})^n$ . This parameter can be tuned to achieve a desirable trade-off between  $P_{\text{repeat}}$  and

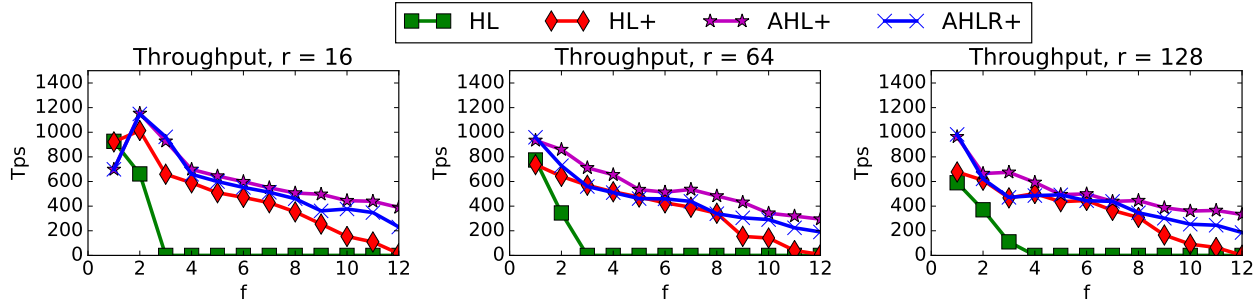


Figure 8: Throughput with optimizations.

Table 4: TCB size (LoC) of different trusted modules.

PoET	S-PoET	AHL	E-AGGRSIGN	E-RANDGEN
1300	1310	780	130	100

the communication overhead, which is  $O(2^{-l}n^2)$ . For example, when  $l = \log(c)$  for some constant  $c$ ,  $P_{\text{repeat}} \approx 0$  and the communication is  $O(n^2)$ . When  $l = \log(n)$ ,  $P_{\text{repeat}} \approx \frac{1}{c}$  and the communication is  $O(n)$ .

**Reduce committee size.** The committee size is an important factor determining the security of a sharding protocol. Specifically, let  $r$  and  $r'$  be the Byzantine threshold that the entire network, and each committee running BFT can tolerate, respectively. The probability that a committee of size  $n'$  contains more than  $f' = r' \cdot n'$  (i.e., security is broken) is given by:

$$P_{\text{fail}} = 1 - \sum_{k=0}^{f'} \binom{n'}{k} r^k (1-r)^{n'-k} \quad (2)$$

Elastico and OmniLedger assume  $r = 0.25$  and  $r' = \frac{1}{3}$ , which means in order to keep  $P_{\text{fail}} \leq 2^{-20}$ ,  $n'$  must be greater than 600. In GRANBEA, each committee runs AHL+, which means  $r' = \frac{1}{2}$ . The result is that  $n'$  becomes significantly smaller. For example, for the same  $P_{\text{fail}} \leq 2^{-20}$ , GRANBEA requires only  $n' \geq 80$ . Smaller committees lead to two benefits, both result in better performance. First, each committee attains higher throughput due to lower communication overhead. Second, there are more committees per network, which increases the overall throughput under light contention between transactions.

## 5. PERFORMANCE EVALUATION

In this section, we present comprehensive evaluations of our proposed optimizations and new design, namely AHL+, S-PoET and GRANBEA. We show that AHL+ has  $7\times$  higher throughput and  $5\times$  lower latency than the original Hyperledger Fabric, and it scales to a large  $f$ . S-PoET reduces the stale block rate by  $4\times$ , which enables it to sustain a high throughput as network size increases. In GRANBEA, committee formation is two orders of magnitude more efficient, and the resulting committees are two orders of magnitude smaller.

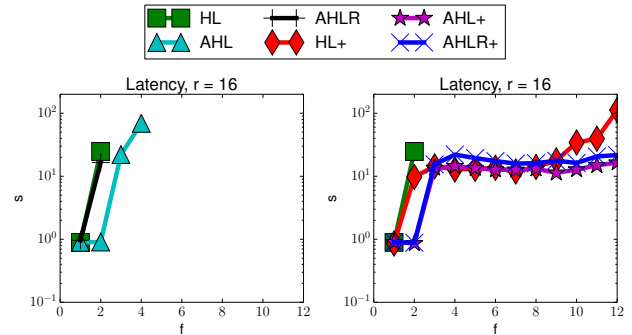


Figure 9: Latency of different HL-based systems.

We quantify the cost of using SGX in terms of security and runtime overhead. Table 4 details the TCB sizes of the trusted components in the protocols. Recall that large TCB implies complications in vetting, it is undesired with regard to security. It can be seen that the enclaves are implemented in less than 1310 lines of code, which is small and hence amenable to formal verification. Table 5 details runtime costs of enclave operations on SGX-enabled processor. The most expensive operations involve public key signatures which signing and signature verification costs about  $450\mu\text{s}$  and  $844\mu\text{s}$ , respectively. Context switching and other symmetric key operations take less than  $5\mu\text{s}$ .

### 5.1 AHL+

We compare AHL+ against several baselines. HL denotes the original Hyperledger Fabric. HL+ is HL with two optimizations discussed in Section 4.2 which are queue separation and removal of request multicast, and AHLR+ is AHL with the two optimizations. Figure 8 shows the throughput of AHL+ and the baselines under the same setup described in Section 3.1.

One observation is that AHL+ performs significantly better than HL. The former continues to offer over 300 tps with  $f = 12$ , whereas the latter crashes as soon as  $f = 4$ . Before HL crashing, at  $f = 3$ , AHL+ achieves  $7\times$  higher throughput. Another observation is that the two optimizations deliver significant improvement, even without the use of trusted hardware. In particular, the throughput of HL+ is close to that of AHL+. However, the former's throughput decreases faster and the system crashes at  $f = 12$ . In

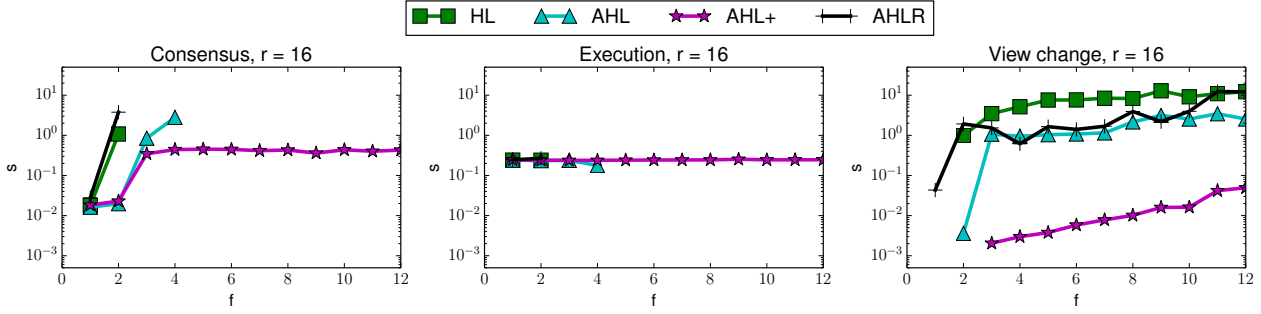


Figure 10: Cost breakdown for different operations per transaction.

Table 5: Runtime costs of enclave operations (excluding enclave switching cost which is roughly  $2.7\mu s$ ).

Operations	Time ( $\mu s$ )
ECDSA Signing	458.4( $\pm 0.4$ )
ECDSA Verification	844.2( $\pm 0.8$ )
SHA256	2.5( $\pm 0.1$ )
AHL Append	5.1( $\pm 0.1$ )
AHL Lookup	465.3( $\pm 0.8$ )
AHL Truncate	2.1( $\pm 0.1$ )
E-AGGRSIGN ( $f = 8$ )	8031.2( $\pm 2.3$ )
E-RANDGEN	482.2( $\pm 0.5$ )
PoET-GetWaitTime	465.2( $\pm 0.5$ )
PoET-GetWaitCertificate	1311.5( $\pm 0.9$ )

other words, trusted hardware is the important factor that prevents the system from crashing. The performance of AHLR+ is even closer to that of AHL+, but it is still worse because of the communication bottleneck at the leader. The latency of these systems are shown in Figure 9. AHL+ always has the lowest latency, whereas those of HL and AHL are only shown before they crash. HL+ maintains relatively low latency, but inflates quickly after  $f = 8$ .

To better understand the difference in the systems’ performances, we examined the cost break down of a transaction. Figure 10 compares the systems in terms of consensus time, execution time, and the time required to complete a view change. It can be seen that the costs of consensus and view change dominate, and those of AHL+ are the lowest. View changes in AHL+ are more than an order of magnitude faster than in other systems. Furthermore, although HL and AHL crash earlier, view changes are still being completed with higher  $f$ . This demonstrates that the systems are stuck in repeated view changes.

## 5.2 S-PoET

We compare S-PoET with the original PoET using the same setting as in Section 3.2. Moreover, we set the bit length of  $q$  to  $l = \frac{\log(n)}{2}$ , which results in the expected effective network size of roughly  $\sqrt{n}$ . We report their throughput

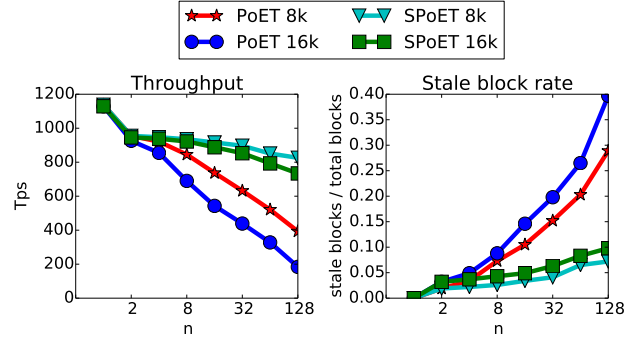


Figure 11: Comparison of PoET and S-PoET throughput and stale block rate.

and stale block rates in Figure 11.

The results demonstrate that S-PoET indeed reduces the stale block rate. As discussed in Section 4.3, this is due to the use of  $q$  to restrict expected number of conflicting blocks. In particular, when  $n = 128$  S-PoET incurs  $4\times$  lower rate than PoET, translating to  $5\times$  higher throughput. For any  $n$ , S-PoET even outperforms PoET when the latter uses smaller blocks. For example, at  $n = 128$ , S-PoET’s throughput is 734 tps using 8MB blocks, whereas PoET’s throughput is 393 tps using 4MB blocks.

## 5.3 GRANBEA

We compare GRANBEA against OmniLedger in terms of committee formation time and the required committee size such that  $P_{\text{fail}} \leq 2^{-20}$  using the same experimental setup as in Section 3.3. In GRANBEA, we set  $l = \log(n) - \log(\log(n))$ , attaining  $O(n \log(n))$  communication overhead while keeping  $P_{\text{repeat}}$  small (below  $2^{-11}$  for  $n = 256$ ). We measure empirically the maximum propagation delay in different network sizes for a 1KB message, and conservatively set  $\Delta$  to be  $3\times$  the measured values. In our experiments,  $\Delta$  ranges from  $2s$  to  $4.5s$ .

**Committee formation.** Figure 12 (left) compares the costs of committee formation in OmniLedger and GRANBEA. It shows that GRANBEA is up to  $35\times$  faster. We attribute this gap to the difference in their communication complexity:  $O(n \log(n))$  versus  $O(nc^2)$ .

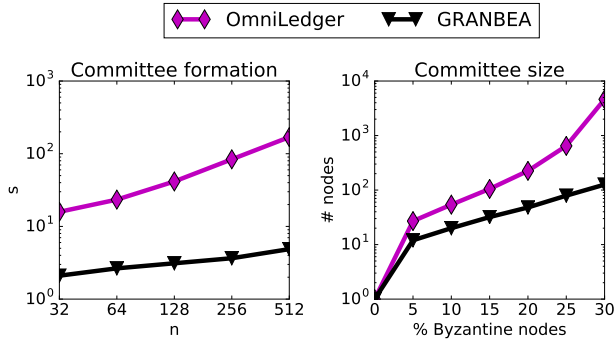


Figure 12: Comparison of committee formation cost and committee size between GRANBEA and OmniLedger [33].

**Committee size.** Figure 12 (right) compares the committee sizes against increasing Byzantine threshold. It can be seen that OmniLedger requires exponentially large committees to tolerate more Byzantine failures. On the other hand, GRANBEA maintains a slower growth, and keeps the committees upto two orders of magnitude smaller.

## 5.4 Discussion of Future Work

This section has demonstrated the effect of our proposed optimizations in improving throughput and scalability of existing blockchain systems. However, the current implementations have two limitations that can be addressed in future work. First, AHL+ does not fully prioritize consensus over request messages. It is not clear whether using a priority queue to always draining the consensus before the request messages will result in better performance. Second, the evaluation does not consider end-to-end performance of GRANBEA. A full-fledged sharding protocol requires many other components, including identity blockchain, two-phase lock/unlock protocol to handle cross-shard transactions, network and execution engine. We plan to re-implement OmniLedger’s design for GRANBEA.

## 6. RELATED WORKS

**Scaling BFT.** Early works on scaling BFT protocols have focused on reducing communication cost [19, 35], number of replicas [18, 39, 61, 29] or execution cost [23]. They either do not use trusted hardware or rely on hardware with limited performance such as smart cards or FPGA. Our work, on the other hand, achieves scalability using Intel SGX.

**Using SGX for distributed consensus.** PoET is one of many consensus protocols that exploit SGX. Hybster [11] also relies on SGX to implement TrInc instances [39]. It focuses on scaling consensus in multi-core settings, and implements a two-phase ordering protocol which can run in parallel. Hybster allows honest nodes to detect equivocation upon receiving conflicting messages, but unlike AHL+, it cannot prevent the malicious node from issuing such conflicting messages. Proof-of-Useful-Work (PoUW) [63] is a variant of PoW that uses SGX to certify that a miner has executed some useful workloads. Instead of solving PoW puzzles, the miners execute some workloads. The execution is measured by the PoUW enclave which issues a leader certificate based on the amount of computation the miner has

completed. Similar to PoET, only nodes with valid certificates can propose a new block. We remark that Hybster and PoUW can serve as other case studies in our work, besides AHL, AHLR and PoET. Given the source code unavailability, we plan to include them in future work.

Microsoft Coco [8] implements the entire consensus protocol in a trusted execution environment, reducing the failure model to crash failure. As a result, more efficient protocols such as Raft [51] and Paxos [38, 37] can be used. However, this approach incurs a much larger TCB than AHL+, making it more vulnerable to exploitation in the software stack. Our work only considers BFT and PoW based protocols. Nevertheless, in our preliminary evaluation of Quorum [28], a similar system that implements Raft consensus, we observed very low throughputs, i.e., less than 200 tps. This poor performance is due to the overhead of the Ethereum software stack used for the non-consensus components.

**Other consensus protocols for blockchains.** Stellar [7] and Ripple [6] assume a federated network setting. A node belong to a federate comprising a set of other nodes that it trusts. Such a federate is called a *quorum slice* in Stellar or a *unique node list* in Ripple. The node only communicates with members of its federate during consensus. Ripple’s underlying consensus is a variant of PBFT. Stellar, on the other hand, proposes a new Byzantine agreement protocol which guarantees that a node ratifies a transaction if and only if its quorum does so. These protocols demonstrate high throughput at large scale, but their security depends on correct federate configuration, which is either non-trivial in large scale or subject to high degree of centralization.

The most popular alternative to PoW in permissionless settings is Proof of Stake (PoS) protocol. In PoS, the nodes are required to stake their resources, e.g., cryptocurrencies, in order to take part in the protocol. PoS protocols can be divided into two types: chain-based and BFT-based [14]. In the former, the node is elected to be a leader based on its stake, and the leader can issue a next block. Examples include [60, 12, 31]. These protocols choose availability over consistency, and their security model is similar to that of PoW. In contrast, BFT-based PoS protocols require nodes to cast votes over multiple rounds. The votes may be weighted based on voters’ stakes. Examples include Tendermint [36], Algorand [45] and Casper [14]. We remark that PoET can be seen as an instance of chain-based PoS wherein every node has equal stake. To our knowledge, there has been no performance study of chain-based PoS, and thus our work offers the first baseline.

The protocols discussed above aim to overcome scalability issues of BFT and PoW. As such, our work can be extended to include them, i.e., they can be evaluated and improved using trusted hardware, which we leave for future work.

**Scaling other component of blockchain.** While consensus protocols have been the main focus of scaling blockchain, improving other parts of the blockchain software stack has been largely ignored. Forkbase [62] is the first storage engine specifically designed with blockchain architecture in mind. It supports analytical queries at more than an order of magnitude lower cost than the current key-value backend. We expect other works that follow to address the potential bottlenecks in the storage and execution engine. While they are orthogonal to our work, the results can be combined to offer a highly scalable blockchain solution.

## 7. CONCLUSIONS

In this paper, we examined three scaling proposals for distributed consensus protocols and showed that there remain scalability limitations. Following the performance evaluation, we propose two design principles which are *scale up by scaling down*, and *prioritize consensus messages*. We then presented optimizations that harness trusted hardware, in particular Intel SGX, to improve upon the state-of-the-art solutions. We demonstrated that the optimizations indeed offer significant performance enhancement over the existing systems. More specifically, a SGX-based PBFT protocol achieves up to  $7\times$  higher throughput than Hyperledger Fabric, and prevents the system from crashing as the network size increases. The optimization over POET enables the system to maintain high throughput at scale. Finally, we proposed a new sharding protocol GRANBEA that improves the shard creation phase by  $35\times$  while keeping the shard sizes order of magnitude smaller in comparison to existing techniques.

## 8. REFERENCES

- [1] Bitcoin energy consumption. <https://digiconomist.net/bitcoin-energy-consumption>.
- [2] Intel SGX SDK for Linux. <https://github.com/01org/linux-sgx>.
- [3] PoET Fork Resolver. [https://github.com/hyperledger/sawtooth-core/blob/master/consensus/poet/core/sawtooth\\_poet/poet\\_consensus/poet\\_fork\\_resolver.py](https://github.com/hyperledger/sawtooth-core/blob/master/consensus/poet/core/sawtooth_poet/poet_consensus/poet_fork_resolver.py).
- [4] Poet specification. <https://sawtooth.hyperledger.org/docs/core/releases/0.8/architecture/poet.html>.
- [5] Proof of elapsed time. <https://sawtooth.hyperledger.org/docs/core/releases/latest/introduction.html>.
- [6] Ripple. <https://ripple.com>.
- [7] Stellar. <https://stellar.org>.
- [8] The Coco Framework. <http://aka.ms/cocopaper>.
- [9] M. Al-Bassam, A. Sonnino, S. Bano, D. Hrycyszyn, and G. Danezis. Chainspace: A sharded smart contracts platform. In *NDSS*, 2018.
- [10] I. Anati, S. Gueron, S. Johnson, and V. Scarlata. Innovative technology for cpu based attestation and sealing. In *Proceedings of the 2nd international workshop on hardware and architectural support for security and privacy*, volume 13. ACM New York, NY, USA, 2013.
- [11] J. Behl, T. Distler, and R. Kapitza. Hybrids on steroids: Sgx-based high performance bft. In *Proceedings of the Twelfth European Conference on Computer Systems*, pages 222–237. ACM, 2017.
- [12] I. Bentov, A. Gabizon, and A. Mizrahi. Cryptocurrencies without proof of work. In *International Conference on Financial Cryptography and Data Security*, pages 142–157. Springer, 2016.
- [13] J. Bonneau, J. Clark, and S. Goldfeder. On bitcoin as a public randomness source. *IACR Cryptology ePrint Archive*, 2015:1015, 2015.
- [14] V. Buterin and V. Griffith. Casper the friendly finality gadget. <https://arxiv.org/abs/1710.09437>.
- [15] M. Castro. *Practical Byzantine Fault Tolerance*. PhD thesis, Massachusetts Institute of Technology, 2001.
- [16] M. Castro, B. Liskov, et al. Practical byzantine fault tolerance. In *OSDI*, volume 99, pages 173–186, 1999.
- [17] L. Chen, L. Xu, N. Shah, Z. Gao, Y. Lu, and W. Shi. On security analysis of proof-of-elapsed-time (poet). In *International Symposium on Stabilization, Safety, and Security of Distributed Systems*, pages 282–297. Springer, 2017.
- [18] B.-G. Chun, P. Maniatis, S. Shenker, and J. Kubiatowicz. Attested append-only memory: Making adversaries stick to their word. In *ACM SIGOPS Operating Systems Review*, volume 41, pages 189–204. ACM, 2007.
- [19] J. Cowling, D. Myers, B. Liskov, R. Rodrigues, and L. Shrira. Hq replication: A hybrid quorum protocol for byzantine fault tolerance. In *Proceedings of the 7th symposium on Operating systems design and implementation*, pages 177–190. USENIX Association, 2006.
- [20] C. Decker and R. Wattenhofer. Information propagation in the bitcoin network. In *Peer-to-Peer Computing (P2P), 2013 IEEE Thirteenth International Conference on*, pages 1–10. IEEE, 2013.
- [21] T. T. A. Dinh, R. Liu, M. Zhang, G. Chen, and B. C. Ooi. Untangling blockchain: a data processing view of blockchain systems. *Transactions of Knowledge Engineering*, 2017.
- [22] T. T. A. Dinh, J. Wang, G. Chen, R. Liu, B. C. Ooi, and K.-L. Tan. Blockbench: A framework for analyzing private blockchains. In *Proceedings of the 2017 ACM International Conference on Management of Data*, pages 1085–1100. ACM, 2017.
- [23] T. Distler and R. Kapitza. Increasing performance in byzantine fault-tolerant systems with on-demand replica consistency. In *Proceedings of the sixth conference on Computer systems*, pages 91–106. ACM, 2011.
- [24] J. R. Douceur. The sybil attack. In *International Workshop on Peer-to-Peer Systems*, pages 251–260. Springer, 2002.
- [25] I. Eyal and E. G. Sirer. Majority is not enough: Bitcoin mining is vulnerable. In *International conference on financial cryptography and data security*, pages 436–454. Springer, 2014.
- [26] A. E. Gencer, S. Basu, I. Eyal, R. van Renesse, and E. G. Sirer. Decentralization in bitcoin and ethereum networks. 2018.
- [27] A. Gervais, G. O. Karame, K. Wüst, V. Glykantzis, H. Ritzdorf, and S. Capkun. On the security and performance of proof of work blockchains. In *Proceedings of the 2016 ACM SIGSAC Conference on Computer and Communications Security*, pages 3–16. ACM, 2016.
- [28] JP Morgan. Quorum. <https://github.com/jpmorganchase/quorum>.
- [29] R. Kapitza, J. Behl, C. Cachin, T. Distler, S. Kuhnle, S. V. Mohammadi, W. Schröder-Preikschat, and K. Stengel. Cheapbft: resource-efficient byzantine fault tolerance. In *Proceedings of the 7th ACM european conference on Computer Systems*, pages 295–308. ACM, 2012.
- [30] J. Katz and Y. Lindell. *Introduction to modern cryptography*. CRC Press, 2014.

- [31] S. King and S. Nadal. Ppcoin: peer-to-peer crypto-currency with proof-of-stake (2012). URL <https://peercoin.net/assets/paper/peercoin-paper.pdf>. [Online], 2017.
- [32] E. K. Kogias, P. Jovanovic, N. Gailly, I. Khoffi, L. Gasser, and B. Ford. Enhancing bitcoin security and performance with strong consistency via collective signing. In *25th USENIX Security Symposium (USENIX Security 16)*, pages 279–296. USENIX Association, 2016.
- [33] E. Kokoris-Kogias, P. Jovanovic, L. Gasser, N. Gailly, and B. Ford. Omniledger: A secure, scale-out, decentralized ledger. *IACR Cryptology ePrint Archive*, 2017:406, 2017.
- [34] R. Kotla, L. Alvisi, M. Dahlin, A. Clement, and E. Wong. Zyzyva: speculative byzantine fault tolerance. In *ACM SIGOPS Operating Systems Review*, volume 41, pages 45–58. ACM, 2007.
- [35] R. Kotla, L. Alvisi, M. Dahlin, A. Clement, and E. Wong. Zyzyva: speculative byzantine fault tolerance. In *ACM SIGOPS Operating Systems Review*, volume 41, pages 45–58. ACM, 2007.
- [36] J. Kwon. Tendermint: Consensus without mining. <https://tendermint.com/static/docs/tendermint.pdf>.
- [37] L. Lamport. Fast paxos. *Distributed Computing*, 19(2):79–103, 2006.
- [38] L. Lamport et al. Paxos made simple. *ACM Sigact News*, 32(4):18–25, 2001.
- [39] D. Levin, J. R. Douceur, J. R. Lorch, and T. Moscibroda. Trinc: Small trusted hardware for large distributed systems. In *NSDI*, volume 9, pages 1–14, 2009.
- [40] S. Liu, P. Viotti, C. Cachin, V. Quéma, and M. Vukolic. Xft: Practical fault tolerance beyond crashes. In *OSDI*, pages 485–500, 2016.
- [41] L. Luu, V. Narayanan, C. Zheng, K. Baweja, S. Gilbert, and P. Saxena. A secure sharding protocol for open blockchains. In *Proceedings of the 2016 ACM SIGSAC Conference on Computer and Communications Security*, pages 17–30. ACM, 2016.
- [42] D. Malkhi and M. Reiter. Byzantine quorum systems. *Distributed Computing*, 11(4):203–213, 1998.
- [43] D. Mazieres. The stellar consensus protocol: A federated model for internet-level consensus. *Stellar Development Foundation*, 2015.
- [44] F. McKeen, I. Alexandrovich, A. Berenzon, C. V. Rozas, H. Shafi, V. Shanbhogue, and U. R. Savagaonkar. Innovative instructions and software model for isolated execution. *HASP@ ISCA*, 10, 2013.
- [45] S. Micali. Algorand: the efficient and democratic ledger. *arXiv preprint arXiv:1607.01341*, 2016.
- [46] S. Micali, M. Rabin, and S. Vadhan. Verifiable random functions. In *Foundations of Computer Science, 1999. 40th Annual Symposium on*, pages 120–130. IEEE, 1999.
- [47] A. Miller and J. J. L. Jr. Anonymous byzantine consensus from moderately-hard puzzles: A model for bitcoin. Technical report, University of Central Florida, 2014.
- [48] A. Miller and J. J. LaViola Jr. Anonymous byzantine consensus from moderately-hard puzzles: A model for bitcoin. Available on line: <http://nakamotoinstitute.org/research/anonymous-byzantine-consensus>, 2014.
- [49] J. Morgan and O. Wyman. Unlocking Economic Advantage with Blockchain. A guide for asset managers, 2017.
- [50] S. Nakamoto. Bitcoin: A peer-to-peer electronic cash system, 2008.
- [51] D. Ongaro and J. K. Ousterhout. In search of an understandable consensus algorithm. In *USENIX Annual Technical Conference*, pages 305–319, 2014.
- [52] R. Pass, L. Seeman, and A. Shelat. Analysis of the blockchain protocol in asynchronous networks. In *Annual International Conference on the Theory and Applications of Cryptographic Techniques*, pages 643–673. Springer, 2017.
- [53] M. Rosenfeld. Analysis of hashrate-based double spending. *arXiv preprint arXiv:1402.2009*, 2014.
- [54] B. Schoenmakers. A simple publicly verifiable secret sharing scheme and its application to electronic voting. In *Annual International Cryptology Conference*, pages 148–164. Springer, 1999.
- [55] D. Schwartz, N. Youngs, A. Britto, et al. The ripple protocol consensus algorithm. *Ripple Labs Inc White Paper*, 5, 2014.
- [56] Y. Sompolinsky and A. Zohar. Secure high-rate transaction processing in bitcoin. <https://eprint.iacr.org/2013/881.pdf>.
- [57] M. Stadler. Publicly verifiable secret sharing. In *International Conference on the Theory and Applications of Cryptographic Techniques*, pages 190–199. Springer, 1996.
- [58] E. Syta, P. Jovanovic, E. K. Kogias, N. Gailly, L. Gasser, I. Khoffi, M. J. Fischer, and B. Ford. Scalable bias-resistant distributed randomness. In *Security and Privacy (SP), 2017 IEEE Symposium on*, pages 444–460. Ieee, 2017.
- [59] E. Syta, I. Tamas, D. Visher, D. I. Wolinsky, P. Jovanovic, L. Gasser, N. Gailly, I. Khoffi, and B. Ford. Keeping authorities “honest or bust” with decentralized witness cosigning. In *Security and Privacy (SP), 2016 IEEE Symposium on*, pages 526–545. Ieee, 2016.
- [60] P. Vasin. Blackcoins proof-of-stake protocol v2. URL: <https://blackcoin.co/blackcoin-pos-protocol-v2-whitepaper.pdf>, 2014.
- [61] G. S. Veronese, M. Correia, A. N. Bessani, L. C. Lung, and P. Verissimo. Efficient byzantine fault-tolerance. *IEEE Transactions on Computers*, 62(1):16–30, 2013.
- [62] S. Wang, T. T. A. Dinh, Q. Lin, Z. Xie, M. Zhang, Q. Cai, G. Chen, W. Fu, B. C. Ooi, and P. Ruan. Forkbase: an efficient storage engine for blockchain and forkable applications. <https://arxiv.org/pdf/1802.04949.pdf>.
- [63] F. Zhang, I. Eyal, R. Escriva, A. Juels, and R. van Renesse. Rem: Resource-efficient mining for blockchains. *IACR Cryptology ePrint Archive*, 2017:179, 2017.

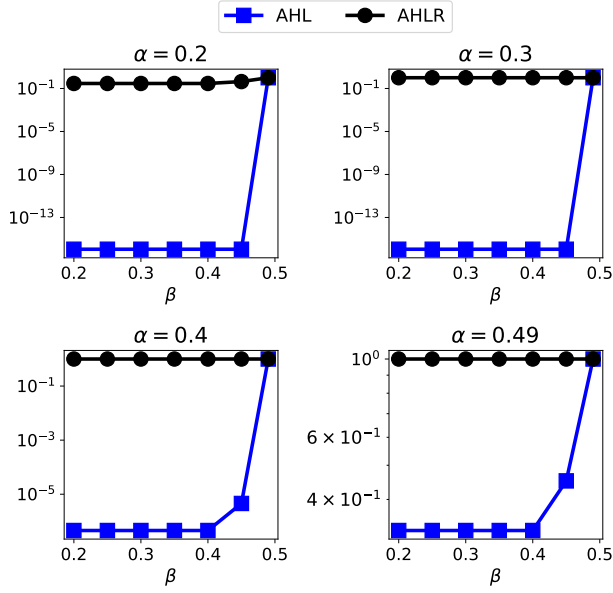


Figure 13: View-change probability of AHL and AHLR w.r.t failure of message deliver.

## APPENDIX

### A. VIEW-CHANGE PROBABILITY OF AHL AND AHLR

Our experiment results show that AHLR’s communication pattern inspired by Byzcoin [32] might have a reverse effect on the throughput if the network communication is not sufficiently robust<sup>6</sup>. In the following, we compare the probability of view-change embodied in AHL and AHLR. We quantify these probabilities in term of message delivery, and show that the latter is more prone to view-change.

**AHL communication.** Under AHL communication pattern, each node sends and receives  $n - 1$  messages in each phase, except for the Pre-prepare phase where in only the leader is multicasting the **pre-prepare** messages. Let us denote by  $\alpha$  the probability that a **pre-prepare** message sent by the leader fails to deliver at a receiving node<sup>7</sup>; by  $\beta$  the probability that a **prepare** or **commit** message multicasted by a node fails to deliver at its destination. For simplicity, we assume that the delivery of one message is independent of another.

Let us denote by  $F(x, n, p)$  and  $CF(x, n, p)$  a cumulative distribution function and a complementary cumulative distribution function of a random variable that follows a binomial distribution  $B(n, p)$ , respectively:

$$F(x, n, p) = \sum_{k=0}^x \binom{n}{k} p^k (1-p)^{n-k}$$

$$CF(x, n, p) = 1 - F(x, n, p)$$

Let  $v = \lfloor \frac{n-1}{2} \rfloor$ . In both AHL and AHLR, the quorum size  $v + 1$ .

The probability  $\mu$  that a quorum has received **pre-prepare** message, yet a node fails to collect a *prepare*

*certificate* (i.e., a quorum of **prepare** messages) is:

$$\mu = F(v, n, \alpha) \times CF(v, n, \beta) \quad (3)$$

The probability  $\epsilon$  that a quorum has received **prepare** message, yet a node fails to collect a *commit certificate* (i.e., a quorum of **commit** messages) is:

$$\epsilon = F(v, n, \mu) \times CF(v, n, \beta) \quad (4)$$

The probability  $\gamma_{AHL}$  that a node requests for a view-change is:

$$\gamma_{AHL} = 1 - (1 - \alpha)(1 - \mu)(1 - \epsilon) \quad (5)$$

The probability that AHL enters view-change is:

$$P_{AHL} = CF(v, n, \gamma_{AHL}) \quad (6)$$

**AHLR communication.** Unlike AHL, the leader in AHLR is tasked to collect messages and distribute a proof that there has been a quorum for a message in question, and each node only needs to communicate with the leader. Let us again denote by  $\alpha$  the probability that a message sent by the leader fails to deliver at a receiving node, and by  $\beta$  the probability that a message sent by a node fails to deliver at the leader.

<sup>6</sup>We note that in Byzcoin’s experimental evaluation, the authors do not take into consideration events of view-change and their cost

<sup>7</sup>More precisely, it is not delivered within the time-out

The probability  $\phi$  that the leader fails to collect a quorum of responses for a message that it has sent is:

$$\phi = F(v, n, \alpha) \times CF(n, v, \beta) \quad (7)$$

The probability  $\omega$  that a node fails to receive a proof that there has been a quorum for **prepare** or **commit** message from the leader is:

$$\omega = \phi + (1 - \phi)\alpha \quad (8)$$

The probability  $\gamma_{AHLR}$  that a node raises a view-change request is:

$$\gamma_{AHLR} = 1 - (1 - \alpha)(1 - \omega)^2 \quad (9)$$

The probability that AHLR enters view-change is:

$$P_{AHLR} = CF(v, n, \gamma_{AHLR}) \quad (10)$$

Figure 13 plot probability  $P_{AHLR}$  and  $P_{AHL}$  with respect to varying  $\alpha$  and  $\beta$ . It can be observe that  $P_{AHLR}$  is consistently higher than  $P_{AHL}$  for almost all  $\alpha$  and  $\beta$  that are lower than  $0.45$ . As these two values approach  $0.5$ , both  $P_{AHLR}$  and  $P_{AHL}$  approach  $1$ . The reason is that when  $\alpha$  and  $\beta$  approach  $0.5$ , the expected number of messages that a node could collect in a particular consensus phase  $p$  reduces sharply to  $\lfloor \frac{n-1}{2} \rfloor$ , preventing it from forming a necessary quorum. This, in turn, forces the node to raise a view change request. Our model suggests that that AHLR communication pattern is less robust than AHL’s all-to-all communication pattern. This makes the former more prone to view changes and deteriorates its throughput when the network is congested.